A model predictive control approach to aircraft motion control

Luca Deori, Simone Garatti, Maria Prandini

Abstract— **We consider the problem of designing a controller that is able to steer an aircraft to some target position, while satisfying a set of constraints originating from physical limitations and comfort requirements. The key idea is to use feedback linearization, and then approximate the constraints in the new state and control variables so as to make them convex. This enables the on-line usage of the model predictive control strategy to aircraft motion control.**

I. INTRODUCTION

In this paper, we develop a novel Model Predictive Control (MPC) scheme for aircraft motion control, where the aircraft is steered from some origin position to a target destination while satisfying constraints related to aircraft physical limitations and passengers comfort. The use of MPC ([18], [16]) is motivated by its well known capability of handling constraints. The main idea behind MPC is that of considering at every time instant a finite-horizon optimal control problem, where a cost function is optimized with respect to the choice of the control input subject to the state/input constraints. Then, only the control input for the current time instant is applied and the same finite-horizon control problem is solved over a 1-step shifted time window (receding horizon).

In the case of the considered aircraft motion problem, the main difficulty in applying MPC rests on the fact that the problem is intrinsically nonlinear, and an appropriate formulation of the constrained optimization problem is required so as to make it simple enough to be solved on-line with the available computational resources. The strategy adopted in this paper is as follows. We first explicitly compute a feedback linearizing control law that holds globally. This has the advantage of making the system dynamics linear with respect to the new state and input variables, so that it can be more easily dealt with in the MPC scheme.

The obtained linear model exactly matches the aircraft dynamics, but in the new coordinates frame the state and input constraints become non-convex and very hard to handle. The next step is the reformulation of these new constraints as convex (possibly linear) constraints by introducing suitable relaxations when necessary. Such relaxations are constructed so as to guarantee that the original constraints are satisfied at least for the initial time instant of the considered time horizon. In this way, though the original constraints may be violated in subsequent time instants by the solution of the finite-horizon control problem, they are never violated in the

receding horizon implementation of MPC. Note that in [10], [15] and [13] aircraft motion control is addressed as well, but the presence of constraints is only partially accounted for.

The idea of using feedback linearization followed by a convexification of the constraints to ease the application of MPC for nonlinear systems is not new as it has been applied in e.g. [19], [24], and [14], while [22] discusses the problem from a general perspective. The contribution of this paper is that of using this methodology in a new problem, to the best of our knowledge never tackled in this way before. We develop specific ad-hoc solutions, especially for what concerns the convexification of the constraints, a problem that still has no general solution.

This paper also prepares the ground for innovative solutions in the Air Traffic Management (ATM) context. Since air traffic is expected to increase rapidly over the next decades, new ATM concepts are needed to exploit more efficiently the airspace and to avoid route congestion and delays. A possible solution that has been proposed in the literature rests on the so-called Target Windows (TWs), [4], which are viewed as key to enable new ATM systems in both the SESAR, [1], and CATS, [2], projects. Each TW is a constraint on the 4-D aircraft trajectory, requiring that a space region, usually a rectangle placed on the boundary between two airspace sectors, is hit within a specified time interval. In perspective, each aircraft will be assigned a sequence of TWs to meet, where the TWs altogether are designed with the twofold objective of better exploiting the airspace capacity and of avoiding conflicts. Coping with TWs constraints in aircraft motion control is not straightforward though, and the MPC scheme here developed seems to be the ideal starting point for further addressing this issue.

Paper structure

The rest of the paper is organized as follows. In Section II we describe the model of the aircraft motion and the constraints on the state and control variables as induced by physical limitations and passengers comfort requirements. In Section III we apply feedback linearization to obtain a linear model, while in Section IV the problem of constraints convexification is addressed. The final finite-horizon optimal control problem is specified in Section V, where considerations on its receding horizon implementation are also provided, focusing on recursive feasibility and computational effort. Some simulation results are reported in Section VI, whereas concluding remarks are drawn in Section VII.

II. MODELING FRAMEWORK

A. Aircraft dynamics

We consider a six-state, flat earth, trimmed, point mass model for the aircraft dynamics. The state variables are given by the position of the aircraft expressed in Cartesian coordinates x, y, z with respect to a fixed frame, the True Air Speed (TAS) of the aircraft V, the heading angle ψ, and the mass m of the aircraft. The inputs of the system are the path angle γ (which is the angle between the flat earth and velocity of the aircraft), the bank angle ϕ (which roughly corresponds to the roll angle), and the engine thrust T. The system evolves according to the following equations

$$
\begin{bmatrix} \dot{x} \\ \dot{y} \\ \dot{z} \\ \dot{V} \\ \dot{\psi} \\ \dot{m} \end{bmatrix} = \begin{bmatrix} V\cos\psi\cos\gamma \\ V\sin\psi\cos\gamma \\ V\sin\gamma \\ -\frac{C_D\rho SV^2}{2m} - g\sin\gamma + \frac{T}{m} \\ \frac{C_L\rho SV}{2m}\sin\phi \\ -\eta T \end{bmatrix}, \quad (1)
$$

where C_D and C_L are the drag and lift coefficients, ρ is the air density (which depends on the altitude z), S is the surface of the wings, g is gravitational acceleration, η is a fuel consumption coefficient. According to [3], the lift coefficient is set equal to $C_L = \frac{2mg}{\rho SV^2\cos\phi}$, so that the weight force is always compensated by the lift force (trimmed condition), while the drag coefficient is given by $C_D = C_{D0} + C_{D2}C_L^2$, where C_{D0} and C_{D2} are suitable coefficients. As a result, the dynamics for the heading angle becomes $\dot{\psi} = \frac{g}{V}\tan\phi$. Equations (1) are further simplified by neglecting the mass dynamics equation that seems to be quite slow with respect to other dynamics. Thus, the final model of the aircraft becomes:

$$
\begin{bmatrix} \dot{x} \\ \dot{y} \\ \dot{z} \\ \dot{V} \\ \dot{\psi} \end{bmatrix} = \begin{bmatrix} V\cos\psi\cos\gamma \\ V\sin\psi\cos\gamma \\ V\sin\gamma \\ -K_D\frac{V^2}{m} - g\sin\gamma + \frac{T}{m} \\ \frac{g}{V}\tan\phi \end{bmatrix}, \quad (2)
$$

where we let $K_D = \frac{C_D\rho S}{2}$.

Admittedly, the present model is derived based on some simplifying assumptions that make it just an approximation of the actual dynamics of an aircraft. Nevertheless, it is worth investigating for the following two reasons:

1) it is customary to use simplified models like (2) when addressing ATM applications, see e.g. [17] and [3];
2) more complex and accurate models can be derived as extensions of (2) so that the achievements of this paper retain validity for enhanced models as well.

B. Constraints

In order to account for physical limitations of the aircraft and comfort of passengers, several constraints both on the state variables and on the input variables have to be considered as follows.

• Vertical Acceleration $\ddot{z}$

$$
-a_N \leq \ddot{z} \leq a_N, \quad (3)
$$

where $a_N = 5$ ft/s$^2 = 5 \cdot 0.3048$ m/s^2.

• True Air Speed V

$$
V_{min} \leq V \leq V_{max}. \quad (4)
$$

V_{min} is related to the stall velocity of the aircraft, [3].

• Longitudinal Acceleration

$$
-a_L \leq \dot{V} \leq a_L, \quad (5)
$$

where $a_L = 2$ ft/s$^2 = 2 \cdot 0.3048$ m/s^2.

• Engine Thrust T

$$
T_{min} \leq T \leq T_{max}. \quad (6)
$$

The limit values for the engine thrust can be computed according to [3] and depend on atmospheric conditions.

• Bank Angle ϕ

$$
-\phi_{max} \leq \phi \leq \phi_{max}. \quad (7)
$$

According to [3] ϕ_{max} can vary from 25° to 45° depending on the type of aircraft.

• Path angle γ

$$
\gamma_{min} \leq \gamma \leq \gamma_{max}. \quad (8)
$$

III. FEEDBACK LINEARIZATION

In this section, we perform the feedback linearization of system (2) so as to obtain a linear model for the aircraft with new input and state variables. The adopted procedure is inspired by [23], where, however, a simpler model of an aircraft in a 2-D airspace is considered. The obtained linear system is then discretized so as to get a model that can be easily used in the MPC framework.

First, we set

$$
T = K_D V^2 + mg\sin\gamma + m\tau, \quad (9)
$$
$$
\varphi = \tan\phi, \quad (10)
$$

so obtaining $\dot{V} = \tau$ and $\dot{\psi} = \frac{g}{V}\varphi$, which are linear equations in the new input variables τ and φ. Note that τ represents the part of the acceleration provided by the engine thrust that is still available once the drag and possibly part of the weight force have been compensated.

If we define new state variables

$$
\begin{array}{lll} x_1 = x & x_2 = y & x_3 = z \\ x_4 = V\cos\psi\cos\gamma & x_5 = V\sin\psi\cos\gamma & x_6 = V\sin\gamma \end{array}
$$

then, the equations governing the system evolution become:

$$
\begin{bmatrix} \dot{x}_1 \\ \dot{x}_2 \\ \dot{x}_3 \\ \dot{x}_4 \\ \dot{x}_5 \\ \dot{x}_6 \end{bmatrix} = \begin{bmatrix} x_4 \\ x_5 \\ x_6 \\ \tau\cos\psi\cos\gamma - V\cos\gamma\sin\psi\frac{g}{V}\varphi - V\cos\psi\sin\gamma\dot{\gamma} \\ \tau\sin\psi\cos\gamma + V\cos\gamma\cos\psi\frac{g}{V}\varphi - V\sin\psi\sin\gamma\dot{\gamma} \\ V\cos\gamma\dot{\gamma} + \tau\sin\gamma \end{bmatrix}.
$$

Now, let

$$
u_1 = \tau\cos\psi\cos\gamma - V\cos\gamma\sin\psi\frac{g}{V}\varphi - V\cos\psi\sin\gamma\dot{\gamma} \quad (11)
$$

$$
u_2 = \tau\sin\psi\cos\gamma + V\cos\gamma\cos\psi\frac{g}{V}\varphi - V\sin\psi\sin\gamma\dot{\gamma} \quad (12)
$$

$$
u_3 = V\cos\gamma\dot{\gamma} + \tau\sin\gamma. \quad (13)
$$

Solving (11) and (12) for τ and φ gives

$$\tau = \frac{1}{\cos\gamma}(\cos\psi u_1 + \sin\psi u_2 + V\sin\gamma\dot\gamma) \qquad (14)$$

$$\varphi = \frac{1}{g\cos\gamma}(-\sin\psi u_1 + \cos\psi u_2). \qquad (15)$$

By reconstructing $\dot\gamma$ from (13), we can rewrite (14) as

$$\tau = \cos\gamma\cos\psi u_1 + \cos\gamma\sin\psi u_2 + \sin\gamma u_3, \qquad (16)$$

which, together with (15),

$$T = K_D V^2 + mg\sin\gamma + m\tau \qquad \phi = \arctan(\varphi),$$

and

$$\gamma = \arcsin\left(\frac{x_6}{V}\right) = \arcsin\left(\frac{u_{3,0} + \int_0^t u_{3,\sigma}d\sigma}{V}\right), \qquad (17)$$

gives the nonlinear feedback making the dynamics of x_1, x_2, x_3, x_4, x_5, x_6 linear with respect to the new inputs u_1, u_2, u_3:

$$\begin{bmatrix} \dot x_1 \\ \dot x_2 \\ \dot x_3 \\ \dot x_4 \\ \dot x_5 \\ \dot x_6 \end{bmatrix} = \begin{bmatrix} 0_{3\times3} & I_3 \\ 0_{3\times3} & 0_{3\times3} \end{bmatrix} \begin{bmatrix} x_1 \\ x_2 \\ x_3 \\ x_4 \\ x_5 \\ x_6 \end{bmatrix} + \begin{bmatrix} 0_{3\times3} \\ I_3 \end{bmatrix} \begin{bmatrix} u_1 \\ u_2 \\ u_3 \end{bmatrix}. \qquad (18)$$

Interestingly, the new state and input variables have a precise physical meaning: the state is composed by the position of the aircraft in Cartesian coordinates (x_1, x_2, x_3) and by the velocity along the Cartesian axes (x_4, x_5, x_6), while the inputs u_1, u_2, u_3 are the accelerations along the x, y, z axes respectively. Note that the original state variables can be recovered from the new ones as follows

$$x = x_1 \qquad y = x_2 \qquad z = x_3 \qquad (19)$$

$$V^2 = x_4^2 + x_5^2 + x_6^2 \qquad (20)$$

$$\psi = \arctan(\frac{x_5}{x_4}). \qquad (21)$$

If we discretize system (18) by applying a constant input in the interval $[t, t+T_s)$, where T_s is the sample time, we get:

$$\mathbf{x}_{t+1} = A\mathbf{x}_t + B\mathbf{u}_t \qquad (22)$$

$$\begin{bmatrix} x_{1,t+1} \\ x_{2,t+1} \\ x_{3,t+1} \\ x_{4,t+1} \\ x_{5,t+1} \\ x_{6,t+1} \end{bmatrix} = \begin{bmatrix} I_3 & T_s I_3 \\ 0_{3\times3} & I_3 \end{bmatrix} \begin{bmatrix} x_{1,t} \\ x_{2,t} \\ x_{3,t} \\ x_{4,t} \\ x_{5,t} \\ x_{6,t} \end{bmatrix} + \begin{bmatrix} \frac{T_s^2}{2}I_3 \\ T_s I_3 \end{bmatrix} \begin{bmatrix} u_{1,t} \\ u_{2,t} \\ u_{3,t} \end{bmatrix}.$$

IV. REFORMULATION OF THE CONSTRAINTS IN THE NEW VARIABLES

In this section, constraints introduced in Section II-B are rewritten as constraints on the new state and input variables introduced in Section III. These constraints are then convexified introducing suitable approximations, paying particular care to the satisfaction of the original constraints, at least at the first time instant.

- Vertical Acceleration
The input u_3 is equal to the vertical acceleration $\ddot z$; therefore the constraint (3) can be straightforwardly written as:

$$-a_N \le u_{3,t+i} \le a_N \qquad i = 0,\ldots,M-1. \qquad (23)$$

- True Air Speed
Since $V^2 = x_4^2 + x_5^2 + x_6^2$, the constraints (4) on the TAS can be rewritten as:

$$x_{4,t+i}^2 + x_{5,t+i}^2 + x_{6,t+i}^2 \le V_{max}^2 \qquad i = 1,\ldots,M \qquad (24)$$

$$x_{4,t+i}^2 + x_{5,t+i}^2 + x_{6,t+i}^2 \ge V_{min}^2 \qquad i = 1,\ldots,M \qquad (25)$$

Constraints (24) are already convex, and their interpretation is that the aircraft velocity[1] lies inside a sphere of radius V_{max}. Constraints (25) are instead concave and require that the aircraft velocity lies outside a sphere of radius V_{min}. To attain convexity, constraints (25) are enforced by requiring that the aircraft velocity stays beyond a plane tangent to sphere of radius V_{min} and oriented according to the initial heading angle ψ_t and path angle γ_t, which are available since $\mathbf{x}_t$ is known, see (17) and (19)-(21). The new constraints can be expressed by means of the linear inequalities

$$\begin{bmatrix} -1 & 0 & 0 \end{bmatrix} R_y R_z \begin{bmatrix} x_{4,t+i} \\ x_{5,t+i} \\ x_{6,t+i} \end{bmatrix} \le -V_{min} \quad i = 1,\ldots,M, \quad (26)$$

where the rotation matrices $R_z(\psi_t)$ and $R_y(\gamma_t)$ are defined as:

$$R_z = \begin{bmatrix} \cos\psi_t & \sin\psi_t & 0 \\ -\sin\psi_t & \cos\psi_t & 0 \\ 0 & 0 & 1 \end{bmatrix} \qquad R_y = \begin{bmatrix} \cos\gamma_t & 0 & \sin\gamma_t \\ 0 & 1 & 0 \\ -\sin\gamma_t & 0 & \cos\gamma_t \end{bmatrix}.$$

Note that (24) and (26) pose a stricter condition than (24) and (25), so that the original constraints are always satisfied. The drawback with (26) is that, having the plane tangent to the sphere of radius V_{min} fixed orientation, for values of TAS close to V_{min}, the aircraft is forced to accelerate in order to turn in the finite horizon problem. However this side-effect is negligible for higher values of the TAS, which correspond to the usual flight conditions. Moreover, thanks to the receding horizon strategy, the plane orientation is recomputed at each time step according the actual values of ψ_t and γ_t, and this drawback is further mitigated in the actual trajectory of the aircraft.

- Longitudinal Acceleration
Since $\dot V = \tau$ and (16), the constraint (5) on the longitudinal acceleration rewrites as:

$$-a_L \le \cos\gamma_{t+i}(\cos\psi_{t+i}u_{1,t+i} + \sin\psi_{t+i}u_{2,t+i} +$$
$$+\tan\gamma_{t+i}u_{3,t+i}) \le a_L \qquad i = 0,\ldots,M-1.$$

Substituting the expressions for γ_{t+i} and ψ_{t+i} as functions of $x_{4,t+i}$, $x_{5,t+i}$, $x_{6,t+i}$, it is easily seen that the constraints are not convex. We decided then to approximate them by fixing the values of the heading angle ψ and of the path

---

[1]Note that the aircraft velocity is a vector with modulus equal to V and orientation given by the heading angle ψ and by the path angle γ. Its Cartesian components are x_4, x_5, x_6.

angle γ to their initial values ψ_t and γ_t, which are available through $\mathbf{x}_t$. This approximation seems to be acceptable for the heading angle cannot vary too much in the considered finite time horizon and $\cos\gamma_{t+i}$ keep close to $\cos\gamma_t \approx 1$, given the limitations on the path angle. This yields

$$-a_L \leq \cos\gamma_t(\cos\psi_t u_{1,t+i} + \sin\psi_t u_{2,t+i} + \qquad (27)$$
$$+\tan\gamma_t u_{3,t+i}) \leq a_L \qquad i = 0,\ldots,M-1,$$

which are linear constraints on u_{t+i}, $i = 0,\ldots M-1$. Notably, for $i = 0$, the constraint on u_t is exactly equivalent to the original one, without any approximation. Thus, thanks to the receding horizon strategy for which at each time step only $\mathbf{u}_t$ is indeed actuated, there is no violation of the original constraint (16) in the actual operation of the aircraft.

- Engine Thrust T

Recalling (6) and (9), the constraint on the engine thrust can be written as

$$\frac{T_{min}}{m} \leq \tau + g\sin\gamma + \frac{K_D}{m}V^2 \leq \frac{T_{max}}{m}$$

Variable τ can be treated as in (27), while $\sin\gamma = \frac{x_6}{V}$, leading to

$$\frac{T_{min}}{m} \leq \cos\gamma_t(\cos\psi_t u_{1,t+i} + \sin\psi_t u_{2,t+i} + \tan\gamma_t u_{3,t+i}) +$$
$$+\frac{g}{V_{t+i}}x_{6,t+i} + \frac{K_D}{m}V_{t+i}^2 \leq \frac{T_{max}}{m}, \qquad i = 0,\ldots,M-1.$$

Unfortunately, the constraints are still non-convex because of the presence of $V_{t+i} = \sqrt{x_{4,t+i}^2 + x_{5,t+i}^2 + x_{6,t+i}^2}$.
A first approximation, based on the presumption that V does not change too much in the finite time horizon, consists in keeping V fixed to its initial value V_t for every $i = 0,\ldots,M-1$:

$$\frac{T_{min}}{m} \leq \cos\gamma_t(\cos\psi_t u_{1,t+i} + \sin\psi_t u_{2,t+i} + \tan\gamma_t u_{3,t+i}) +$$
$$+\frac{g}{V_t}x_{6,t+i} + \frac{K_D}{m}V_t^2 \leq \frac{T_{max}}{m}, \quad i = 0,\ldots,M-1. \qquad (28)$$

A second approach, instead, consists in replacing V_{t+i} with worst-case predictions along the considered horizon, where worst-case predictions are computed by recalling that $V_{t+1} = V_t + T_s\tau_t$ and by taking into account the constraints (5) and (4). Precisely, the maximal decrease of the TAS is

$$V_{t+i}^{wc^-} = \max\{V_t - iT_s a_L, V_{min}\} \quad i = 0,\ldots,M, \qquad (29)$$

while the maximal increase is

$$V_{t+i}^{wc^+} = \min\{V_t + iT_s a_L, V_{max}\} \quad i = 0,\ldots,M. \qquad (30)$$

In this case the approximate constraints on the engine thrust would write:

$$\frac{T_{min} - K_D(V_{t+i}^{wc^+})V_{t+i}^{wc^-2}}{m} \leq \qquad (31)$$
$$\cos\gamma_t(\cos\psi_t u_{1,t+i} + \sin\psi_t u_{2,t+i} + \tan\gamma_t u_{3,t+i}) + \frac{g}{V_t}x_{6,t+i}$$
$$\leq \frac{T_{max} - K_D(V_{t+i}^{wc^-})V_{t+i}^{wc^+2}}{m}, \quad i = 0,\ldots,M-1.$$

We do not use worst case predictions for the TAS in the term $\frac{g}{V}x_6$ because the sign of x_6 is unknown, moreover the constraints would result to be excessively conservative. Remarkably, both (28) and (31) are linear constraints, and are such that the first constraint corresponding to $i = 0$ is exactly equivalent to the original constraint on the engine thrust. Thus, again, thanks to the receding horizon strategy, the actual operation of the aircraft satisfies (9).

The constraints (31) are closer to the original constraints than (28), and using (31) it is more likely that the original constraint on the engine thrust is satisfied over the whole finite horizon. Yet, in many cases (31) are too conservative and simulations reveal that the constraints (28) lead to better performance.

- Bank Angle ϕ

The constraint (7) on the bank angle presents a structure similar to that of the constraints on the longitudinal acceleration, that is, on τ. Indeed, by (10) and (15), (7) can be rewritten as:

$$\tan\phi_{min} \leq \frac{1}{g\cos\gamma_{t+i}}(-\sin\psi_{t+i}u_{1,t+i} + \cos\psi_{t+i}u_{2,t+i}) \leq$$
$$\leq \tan\phi_{max} \qquad i = 0,\ldots,M-1.$$

Similarly to (27), the values of γ and ψ are fixed to their initial value γ_t and ψ_t in order to recover linear constraints with respect to the variables $\mathbf{u}$. We have

$$\tan\phi_{min} \leq \frac{1}{g\cos\gamma_t}(-\sin\psi_t u_{1,t+i} + \cos\psi_t u_{2,t+i}) \leq \qquad (32)$$
$$\leq \tan\phi_{max} \qquad i = 0,\ldots,M-1.$$

Note that the constraint on $\mathbf{u}_t$ at $i = 0$ is exactly equivalent to the original constraints on the bank angle, so that the actual aircraft operation satisfies (7) thanks to receding horizon.

- Path Angle γ

Recalling that $x_6 = V\sin\gamma$ the constraint (8) writes as

$$V_{t+i}\sin\gamma_{min} \leq x_{6,t+i} \leq V_{t+i}\sin\gamma_{max} \qquad i = 1,\ldots,M, \quad (33)$$

which is however non-convex due to $V_{t+i} = \sqrt{x_{4,t+i}^2 + x_{5,t+i}^2 + x_{6,t+i}^2}$. Similarly to the case of the engine thrust, (33) can be approximated by keeping V fixed to its initial value V_t for all $i = 1,\ldots,M$, leading to

$$V_t\sin\gamma_{min} \leq x_{6,t+i} \leq V_t\sin\gamma_{max} \quad i = 1,\ldots,M, \qquad (34)$$

or, otherwise, we can replace V_{t+i} with its worst-case prediction computed in (29) and (30). Note that being $\sin\gamma_{min}$ negative and $\sin\gamma_{max}$ positive the worst-case is achieved when V decreases. In this case the constraints on the path angle can be approximated as:

$$V_{t+i}^{wc^-}\sin\gamma_{min} \leq x_{6,t+i} \leq V_{t+i}^{wc^-}\sin\gamma_{max} \quad i = 1,\ldots,M. \quad (35)$$

Note that (34) does not guarantee the satisfaction of the original constraint (8), not even for $i = 1$ because V_t is considered in place of V_{t+1}. Instead, (35) is such that the original constraint is satisfied along the whole finite horizon, and hence the satisfaction of (8) is guaranteed in receding horizon too. Although (35) poses stricter conditions than

(8), simulations reveal that (35) works pretty well and, in view of the previous discussion, it has to be preferred.

V. COST FUNCTION AND OPTIMIZATION PROBLEM

The quadratic cost function to minimize at each time instant t is chosen as follows

$$J = \sum_{i=1}^{M}(\mathbf{x}_{t+i} - \mathbf{x}_{ref})^T S(\mathbf{x}_{t+i} - \mathbf{x}_{ref}) + \sum_{i=0}^{M-1}\mathbf{u}_{t+i}^T R\mathbf{u}_{t+i},$$

where $\mathbf{x}_{ref}$ represent the target (e.g. a final position) that the aircraft is required to reach. The weighting matrix R accounts for fuel consumption and comfort and is chosen as

$$R = R_{rot}^T R_{nor}^T R_d R_{nor} R_{rot},$$

$$R_{rot} = \begin{bmatrix} \cos\psi_t & \sin\psi_t & 0 \\ -\sin\psi_t & \cos\psi_t & 0 \\ 0 & 0 & 1 \end{bmatrix} R_{nor} = \begin{bmatrix} \frac{1}{a_L} & 0 & 0 \\ 0 & \frac{1}{g\tan\phi_{max}} & 0 \\ 0 & 0 & \frac{1}{a_N} \end{bmatrix}.$$

Most precisely, R_{rot} is a rotation matrix that transforms u_1 and u_2 (namely, the accelerations along the x and y axes) into the longitudinal and lateral accelerations with respect to the initial value of the heading angle ψ_t, whereas R_{nor} is a normalization matrix, chosen accordingly to the limits on accelerations. This way, the matrix R_d allows one to weight the longitudinal and lateral accelerations, as well as the vertical acceleration, which are directly related to fuel consumption and comfort.

The matrix S is instead chosen so that the aircraft is properly steered from the initial condition to the target. We use

$$S = S_{rot}^T S_d S_{rot},$$

where S_{rot} is a rotation matrix as R_{rot}, but for an angle $\xi = \arctan(\frac{y-y_{ref}}{x-x_{ref}})$. This way, the matrix S_d weights the position mismatch along the current track of the aircraft and its orthogonal direction (cross-track error). When the aircraft heads exactly in the opposite direction with respect to the target position (so that the cross-track error is 0), a small variation to the angle ξ is artificially added so as to foster the aircraft steering toward the target.

Given the discrete-time model of Section III, the convex constraints discussed in Section IV, and the cost function just introduced, the optimization problem over the finite time horizon is as follows:

$$\min_{\substack{\mathbf{u}_{t+i} \ i=0...M-1}} J \qquad (36)$$
$$\text{s.t.} \begin{cases} \text{dynamics} & (22) \\ \text{constraint} & (23)\ (24)\ (26)\ (27)\ (28)\ (32)\ (35) \end{cases}.$$

According to the receding horizon strategy, only the first computed control action is applied each time and the optimization is repeated at each time step. In this respect, two comments are in order, the first regarding recursive feasibility, the second regarding computational effort.

a) Recursive feasibility: as long as γ_{min} and γ_{max} are suitably chosen close enough to 0, as it happens in standard settings, the introduced constraints are always satisfied by the solution $\mathbf{u}_{t+i} = 0$ $i = 0,\dots,M-1$, which corresponds to keeping the aircraft flying with its current TAS, heading and path angle. This guarantees the feasibility of the finite horizon optimization problem to be solved at each time instant t.

b) Computational effort: the optimization problem (36) to be solved at each time instant t is convex with a quadratic cost function and few constraints, most of which are linear. The number of optimization variables is $3M$, which for standard sampling times T_s between 1 and 5 seconds with a look-ahead time horizon between 20 and 60 seconds is usually not bigger than 60. On a laptop with an Intel Core i7-3630QM CPU and 8Gb of RAM, equipped with an IBM ILOG CPLEX solver, the solution of (36) with $M = 12$ and $T_s = 5$ seconds required about 0.6 seconds, a performance which is compatible with an on-line implementation.

VI. NUMERICAL RESULTS

In this section, we report some numerical results obtained from a simulation, whose purpose was to evaluate the impact of the introduced approximation in the constraints. In the simulation, the aircraft initial state was $\mathbf{x}_0 = [30\ 30\ 3\ 600\ 400\ 0]^T$ (positions are in km, velocities in km/h), and we set $\mathbf{x}_{ref} = [0\ 0\ 0\ 0\ 0\ 0]^T$, $R_d = 0_{3\times3}$, and

$$S_d = \begin{bmatrix} I_3 & 0_{3\times3} \\ 0_{3\times3} & 0_{3\times3} \end{bmatrix}.$$

This means that the aircraft was required to fly from $\mathbf{x}_0$ to the origin of the reference frame, while there was no penalization of the input. We also set the horizon $M = 12$ and $T_s = 5$s. The aim of the simulation was to evaluate whether by means of the constraints in Section IV the aircraft is actually driven along a physically feasible trajectory, while achieving at the same time a good performance in approaching the target. Note that at the beginning the aircraft has the wrong heading with respect to the target. Thus, we expect that the controller makes the aircraft steer. Moreover, the aircraft should descend from the initial altitude to the 0 level on the z axis. Once the target is reached, we expect the aircraft to fly around it, since the TAS cannot drop below V_{min}.

The results achieved by implementing the MPC approach of this paper to the present problem are reported in Figure 1, where both 2-D and 3-D views of the actual trajectory of the aircraft, along with the finite horizon solutions computed at each step, is depicted. In the simulations of the controlled system we added wind disturbance to test its robustness. Following [11], [15], the wind is modeled by adding a stochastic disturbance (w_x, w_y, w_z) to the aircraft velocity along the x, y, z axes respectively. As it appears, the path followed by the aircraft is quite what we expected, and, moreover, the original constraints are all satisfied along the whole aircraft trajectory. Though the approximation introduced to attain convexity hampers the finite horizon solution to make rapid turns, it seems that this approximation does not adversely affect the actual behavior of the aircraft, thanks to the beneficial effect of the receding horizon.
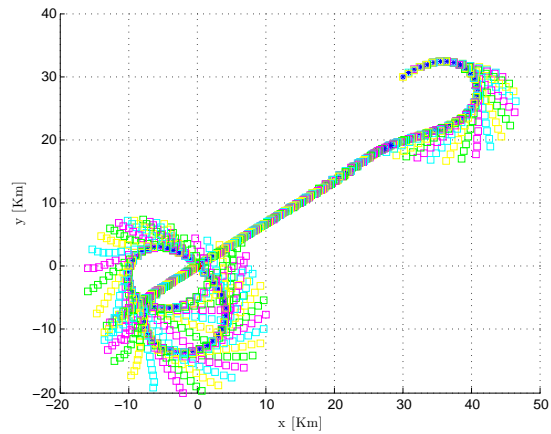
(a) x-y view
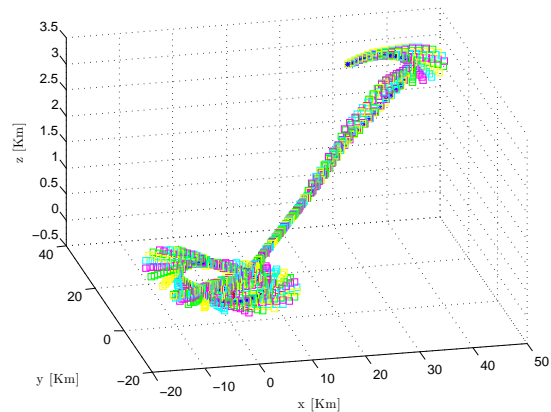
(b) 3D view

Fig. 1: In blue stars the actual receding horizon trajectory of the aircraft, in colored squares the finite horizon solutions computed at each time step.

VII. Conclusions and future work

In this paper, we have developed an MPC controller of the motion of an aircraft that explicitly accounts for constraints arising from physical limitations and comfort requirements. Much effort has been devoted to guarantee the convexity of the constrained optimization problem that has to be repeatedly solved according to the receding horizon strategy. The resulting control algorithm has limited computatical cost and is amenable of on-line implementation.

Further developments that are currently under study concern the extension of the proposed framework to 4-D trajectory management operations, where 4-D constraints have to be imposed to the aircraft trajectory e.g. through Target Windows, [4], and to the case when the aircraft motion is affected by uncertainty due to the presence of wind, [21], [5], [6], [12], [8]. The concurrence of stochastic disturbances and constraints on the aircraft trajectory compels to consider probabilistic constraints, lifting the complexity of problem (36). To the purpose of keeping the overall approach computationally feasible, we envisage the use of the so-called scenario approach, [7], [20], [9], a recently developed randomized method to approximately solve chance-constrained optimization problems.

References

[1] SESAR The ATM Target Concept - Deliverable D3. http://www.eurocontrol.int/sesar/public/standard_page/ documentation.html, December 2006.

[2] CATS State of the Art - Deliverable D1.1. http://www.cats-fp6.aero/cats-fp6/public_deliverables.html, June 2008.

[3] Eurocontrol experimental center. user manual for the base of aircraft data (BADA) revision 3.10. http://www.eurocontrol.int/sites/default/files/content/documents/sesar/bada3.10-user-manual.pdf, 2010.

[4] Report on Target Window Modelling - Deliverable D2.2.4.3. http://www.cats-fp6.aero/cats-fp6/public_deliverables.html, June 2010.

[5] S.G. Benjamin, B.E. Schwartz, and R.E. Cole. Accuracy of acars wind and temperature observations determined by collocation. *Weather & Forecasting*, 14(6), 1999.

[6] S.G. Benjamin, B.E. Schwartz, E.J. Szoke, and S.E. Koch. The value of wind profiler data in us weather forecasting. *Bulletin of the American Meteorological Society*, 85(12), 2004.

[7] M.C. Campi, S. Garatti, and M. Prandini. The scenario approach for systems and control design. *Annual Reviews in Control*, 33(2):149–157, 2009.

[8] G. Chaloulos and J. Lygeros. Effect of Wind Correlation on Aircraft Conflict Probability. *AIAA Journal of Guidance, Control, and Dynamics*, 30(6):1742–1752, 2007.

[9] L. Deori, S. Garatti, and M. Prandini. Stochastic constrained control: trading performance for state constraint feasibility. In *Proceedings of the 2013 European Control Conference*, 2013.

[10] W. Glover and J. Lygeros. A stochastic hybrid model for air traffic control simulation. In *Hybrid Systems: Computation and Control*, pages 372–386. Springer, 2004.

[11] W.n Glover and J. Lygeros. A multi-aircraft model for conflict detection and resolution algorithm evaluation. *HYBRIDGE Deliverable D*, 1, 2004.

[12] J. Hu, M. Prandini, and S. Sastry. Aircraft conflict prediction in presence of a spatially correlated wind field. *IEEE Transactions on Intelligent Transportation Systems*, 6(3):326–340, 2005.

[13] M. R. C. Jackson, V. Sharma, C. M. Haissig, and M. Elgersma. Airborne technology for distributed air traffic management. In *Decision and Control, 2005 and 2005 European Control Conference*. IEEE, 2005.

[14] D.A. Joosten, T.J.J. van den Boom, and T.J.J. Lombaerts. Computationally efficient use of MPC and dynamic inversion for reconfigurable flight control. In *Proceedings of the AIAA Guidance, Navigation and Control Conference and Exhibit*, Honolulu, Hawaii, August 2008.

[15] I. Lymperopoulos. *Sequential Monte Carlo methods in air traffic management*. PhD thesis, Diss., Eidgenössische Technische Hochschule ETH Zürich, Nr. 19004, 2010, 2010.

[16] J.M. Maciejowski. *Predictive control: with constraints*. Pearson education, 2002.

[17] K. Margellos and J. Lygeros. Toward 4D Trajectory Management in Air Traffic Control: A Study Based on Monte Carlo Simulation and Reachability Analysis. *IEEE Transactions on Control Systems Technology*, 21(5):1820–1833, September 2013.

[18] D.Q. Mayne, J.B. Rawlings, C.V. Rao, and P. Scokaert. Constrained model predictive control: Stability and optimality. *Automatica*, 36(6):789–814, 2000.

[19] Kurtz M.J and Henson M.A. Input-output linearizing control of constrained nonlinear process. *Journal of Process Control*, 7(1):3–17, 1997.

[20] M. Prandini, S. Garatti, and J. Lygeros. A randomized approach to stochastic model predictive control. In *Proceedings of the 51st IEEE Conference on Decision and Control*, pages 7315–7320, 2012.

[21] B. Schwartz and S.G. Benjamin. A comparison of temperature and wind measurements from acars-equipped aircraft and rawinsondes. *Weather and forecasting*, 10(3):528–544, 1995.

[22] D. Simon, J. Löfberg, and T. Glad. Nonlinear model predictive control using feedback linearization and local inner convex constraint approximations. In *Proceedings of the 2013 European Control Conference*, pages 2056–2061, 2013.

[23] D.M. Stipanović, G. Inalhan, R. Teo, and C.J. Tomlin. Decentralized overlapping control of a formation of unmanned aerial vehicles. *Automatica*, 40(8):1285–1296, 2004.

[24] W.R. Van Soest, Q.P. Chu, and J.A. Mulder. Combined feedback linearization and constrained model predictive control for entry flight. *Journal of Guidance, Control, and Dynamics*, 29(2):427–434, 2006.